Molecular Crystals and Liquid Crystals
Publication details, including instructions for authors and subscription information:
http://www.tandfonline.com/loi/gmcl16

Structure-Dependent Feature of Electron Transport in Langmuir Multilayer Assemblies

Michio Sugi [a], Tsunekatsu Fukui [a] & Sigeru Iizima [a]
[a] Electrotechnical Laboratory, 5-4-1 Mukodai, 188, Tanashi, Tokyo, Japan
Version of record first published: 21 Mar 2007.

To cite this article: Michio Sugi , Tsunekatsu Fukui & Sigeru Iizima (1979): Structure-Dependent Feature of Electron Transport in Langmuir Multilayer Assemblies, Molecular Crystals and Liquid Crystals, 50:1, 183-200

To link to this article: http://dx.doi.org/10.1080/15421407908084426

Mol. Cryst. Liq. Cryst., 1979, Vol. 50, pp. 183–200

Printed in Holland

Structure-Dependent Feature of Electron Transport in Langmuir Multilayer Assemblies

MICHIO SUGI, TSUNEKATSU FUKUI, and SIGERU IIZIMA

Electrotechnical Laboratory, 5-4-1 Mukodai, 188 Tanashi, Tokyo, Japan

(*Received June 16, 1978*)

The behavior of dc and ac conductivities is studied in the Langmuir multilayer films sandwiched between aluminium electrodes. The structure-dependence of conductivities has been systematically examined on different film structures constructed by the Molecular Assembly Technique. The constituent monolayers used were Cd salts of fatty acids CH_3—$(CH_2)_{n-2}$—COOH with $n = 16, 18, 20$ and a mixture $(C_{16})_x$—$(C_{20})_{1-x}$. The structure dependent aspects are summarized in the following items, which are reasonably interpreted by the model based on the hopping or thermally assisted tunneling of electrons via localized states assumed at each monolayer interface:

1) exponential decrease of dc conductivity with increasing chain length of the fatty acid radical;

2) the same exponential variation of dc conductivity for mixed monolayers;

3) reduction of dc conductivity caused by one single C_{20} monolayer introduced into C_{16} multilayer system;

4) frequency-dispersion of conductivity in heterogeneous multilayer assemblies in accordance with the theoretical prediction.

1 INTRODUCTION

The designed arrangement of molecules is a valuable tool for research in the molecular sciences. This will enable to construct organized molecular system, such as seen in living cells, in which the constituents cooperate with each other to realize a variety of stereo-specific functions.

Multilayer assemblies are constructed using the Langmuir-Blodgett technique[1] by depositing an arbitrary number of monolayers one on top of the other following a planned sequence. The original Langmuir–Blodgett technique comprises manipulation of a monolayer of fatty acid or its salt upon a water–air interface followed by transfer onto a substrate which is dipped and raised through the interface.

On this basis, Kuhn and his co-workers have developed the Molecular Assembly Technique,[2] with which various "heterogeneous assemblies" with deliberately designed sequences of different constituent monolayers can now be constructed as well as the usual Langmuir films or the "homogeneous assemblies."

The studies of charge carrier transport in the multilayer system started as early as in the 1930's.[3] The earlier studies, however, seem to have treated the system as a continuous medium, only making use of the designable thickness given as an integer multiple of the monolayer thickness. The structure in the molecular arrangement was therefore neglected and, consequently, no systematic examination was carried out as to what extent the electrical properties were related to the structure of molecular dimension. Another fatal point was the use of rather unstable monolayers such as Ba and Ca salts or even free acids, which are now known to be apt to undergo structural change during or soon after the deposition,[4] quite in contrast to Cd salt Y-type films, each characterized with a well-defined bilayer *d*-spacing and the nearly hexagonal order of molecular chains.[5]

As for the treatment of the superstructure in the monolayer sequence, the only exception among the earlier reports is a paper of Nathoo and Jonscher,[6] who discussed the possibility of the bilayer hopping of electrons via localized states assumed to locate at every other interface of the multilayer system. The use of free acid monolayers, however, resulted in a poor reproducibility of electrical measurements, which prevented them from further elucidation.

In recent years, a series of papers have been released aiming to clarify the relation between the structure and the carrier transport in order to characterize Cd salt monolayers, i.e., the standard constituents in the multilayer assembly construction.[7-14] It was found that the bilayer hopping is not the case with the Cd salt system, and that the transport is rather explained as the single-layer process, suggesting the existence of localized states at each interface.

The present paper gives a summary of the structure-dependent feature of carrier transport observed in the Cd-salt multilayer system without dye-sensitizers together with a review of the single-layer hopping model by which the experimental results are interpreted.

2 OUTLINE OF THE THEORY

In this section, a review is given for the hopping model, which is based on the following assumptions:

1) each constituent monolayer is associated with localized electronic states at both interfaces, disregarding the difference between the hydrophilic and hydrophobic interfaces in the *Y*-type multilayers;

2) the charge transport is the hopping conduction of electrons via those interface states;

3) each hopping event is characterized with a single rate determined by the interface separation and the electron energy.

The hopping rate is estimated on these assumptions by applying a Mott-type variable range scheme[15] to the monolayers.

The conductivity of the multilayer system is calculated by employing the extended Montroll–Weiss formalism.[16] The nearest neighbor approximation is adopted in the calculation, and, therefore, the single-layer process alone is taken into account.

2.1 The most probable hopping rate

As already given in the previous papers,[8,12] the hopping rate can be estimated starting from a Miller–Abrahams-type expression,[17]

$$\lambda = \lambda_0(2\alpha R)^{3/2} \exp(-2\alpha R - \Delta/kT), \tag{1}$$

where α, R and Δ are the wave function damping constant, the hopping distance and the hopping energy, respectively, and k is the Boltzmann constant, T the absolute temperature. The most probable rate should be resulted from a compromise between the smallest Δ and the shortest R, which are correlated with each other as function of the interface state density N' around the Fermi level and the interface separation l. This situation is described by the application of the variable range mechanism,[15] and we obtain,

$$\Delta_m = (\alpha kT/\pi N' l)^{1/2}, \tag{2}$$

and,

$$R_m = l + \frac{r_m^2}{2l} = l + \frac{1}{2}(1/\pi N'\alpha lkT)^{1/2}, \tag{3}$$

as the most probable values, where the suffix m refers to the most probable value of each variable, and r_m is the radius of hopping domain within which the electron is likely to find a state to hop into.

The most probable rate is given as

$$\lambda_m = \lambda_0(2\alpha l)^{3/2} \exp[-2\alpha l - (4\alpha/\pi N' lkT)^{1/2}], \tag{4}$$

using Eqs. (1)–(3).

As shown in a previous work,[11] the above equations are extended for the mixed monolayers involving different chain lengths. Two extreme cases are considered:

a) the local compositions within the hopping domains are identical everywhere in the monolayer, the homogeneous mixing case;

b) the monolayer is subjected to the large scale fluctuation of local composition, the phase separated case.

In case a), it has been shown that Eqs. (2)–(4) are valid if l is replaced with the average $\langle l \rangle$, and that the hopping process is characterized by a single rate, while in case b) different rates are involved in the process.

2.2 The frequency-behavior of conductivity

A generalized expression of conductivity is given by the well-known fluctuation-dissipation theorem[18] as,

$$\sigma(\omega) = e^2(\partial n/\partial \zeta)_T \, Re D(\omega), \tag{5}$$

where e, n and ζ are the unit charge, the carrier concentration and the chemical potential, respectively, and $D(\omega)$ is the Fourier transform of the diffusion coefficient.

Scher and Lax[16] apply this theorem to a system of non-interacting carriers obeying Boltzmann statistics,

$$(\partial n/\partial \zeta)_T = n/kT, \tag{6}$$

and derive the expression,

$$D(\omega) = \frac{(i\omega)^2}{2} \int_0^\infty \frac{1}{3} \langle [\bar{r}(t) - \bar{r}(0)]^2 \rangle e^{-i\omega t} \, dt. \tag{7}$$

In Eq. (7), $\bar{r}$ is the position vector and the angular brackets denote the ensemble average. They then introduce the Montroll–Weiss formalism[19] for continuous time random walk on a discrete lattice.

In the previous paper,[13] we have studied the frequency-behavior of conductivity in the multilayer assemblies by applying the theory of Scher and Lax in the reduced dimensionality in the system. For heterogeneous assemblies, a frequency dispersion of the conductivity has been predicted as characteristic of each superstructure in the layer sequence, while the homogeneous assemblies or usual Langmuir films have been found to show a frequency-independent conductivity. The dispersion frequency, in contrast to the Maxwell-Wagner-type interface polarization, has been immediately related to the single-layer hopping rate.

The conductivity expression is easily extended to the larger unit cells of monolayer sequence. If the unit cell of a heterogeneous assembly is constructed by depositing M_1 monolayers with the larger rate λ_1 and then M_2 monolayers with smaller rate $\lambda_2 (\lambda_1 \gg \lambda_2)$ for carriers near the Fermi level,

the conductivity in dark is approximated as,

$$\sigma(\omega) = \frac{M_1 + M_2}{M_2}\sigma_2 + \frac{M_1}{M_1 + M_2}\sigma_1 \frac{[c(M_1)\omega/\lambda_1]^2}{1 + [c(M_1)\omega/\lambda_1]^2}, \tag{8}$$

where $c(M_1)$ is evaluated as,[14]

$$c(M_1) = 0.103\, M_1^2 + 0.189\, M_1 + 0.207, \tag{9}$$

and σ_1 and σ_2 are the frequency-independent conductivities of the corresponding homogeneous assemblies, respectively, each given by Eq. (5) using,

$$D(\omega) = l^2\lambda. \tag{10}$$

The dielectric constant $\varepsilon(\omega)$ is given as,

$$\varepsilon(\omega) = \varepsilon(\infty) + \frac{M_1}{M_1 + M_2} \frac{c(M_1)/\lambda_1}{1 + [c(M_1)\omega/\lambda_1]^2}, \tag{11}$$

by means of the Kramers–Kronig relation, where $\varepsilon(\infty)$ refers to the value for $\omega \gg \lambda_1/c(M_1)$.

2.3 The averaging mechanisms

The effect of inhomogeneities in the assemblies has been considered also in the previous work,[13] since the actual assembly system is inevitably associated with occasional structural and compositional imperfections. It has been deduced that the single-rate scheme is apparently held even in the phase-separated case, and that the conductivity by the same Eq. (10), if the rate λ is replaced by the average $\langle\lambda\rangle$. The conductivity can therefore be written as,

$$\sigma \cong \sigma(\langle\lambda\rangle) \cong \langle\sigma(\lambda)\rangle, \tag{12}$$

if we neglect the difference of l in other terms than $\exp(-2\alpha l)$.

The conductivity expression for the homogeneous mixing case is, however, approximated as,

$$\sigma \cong \sigma[\lambda(\langle l\rangle)], \tag{13}$$

with reference to Eq. (4), or rather as,

$$\log\sigma \cong \langle\log\sigma(\lambda)\rangle, \tag{14}$$

since in the realistic case the dominant term is $\exp(-2\alpha l)$.

Two different averaging mechanisms are discriminated from each other. Eq. (12) will give larger conductivity than Eq. (14), since the arithmetic average is always larger than the geometrical average if the variable is associated with a non-zero deviation.

3 EXPERIMENTAL

3.1 Sample preparation

The capacitor-type junctions were fabricated employing the Molecular Assembly Technique.[2]

The substrate, each 1/4 (13 mm × 38 mm, 1.2 mm thick) of an ordinary slide glass, were after a preliminary ultrasonic cleaning, put in a saturated solution of KOH in ethanol for 4 ~ 5 hours, rinsed with bidistilled water in an ultrasonic bath, and then dried in a hot ambient (80 ~ 85°C).

The base and top electrodes were Al (99.9999 %) vacuum-evaporated films formed on the substrate under a pressure $< 10^{-5}$ Torr before and after the monolayer deposition, respectively.

Three junctions were formed on each substrate as shown in Figure 1. Type (a) samples with the contact area of 0.200 ± 0.003 cm^2 were used for dc and low frequency ac measurements, while type (b) samples were for the measurements at frequencies $\geqq 30$ Hz. In the following text, the samples to be referred are of type (a) unless it is otherwise mentioned.

All multilayers to be referred are *Y*-type films formed by alternate stacking of hydrophilic-to-hydrophilic and hydrophobic-to-hydrophobic contacts of monolayers. The Cd salt monolayer was prepared by spreading a 5×10^{-3} M solution of the fatty acid in chloroform (spectro-grade, Tokyo Kasei Co., Tokyo, Japan) on a subphase of 4×10^{-4} M $CdCl_2$ in bidistilled water. The acids used were *n*-carboxylic acids CH_3–$(CH_2)_{n-2}$–COOH with $n = 16$, 18 (palmitic and stearic acids for gas chromatography from Fluka AG, Buchs, Switzerland) and 20 (Arachidic acid (synthetic) from Eastmann Kodak Co., Rochester, U.S.), each of which will be referred by the abbreviation C_n in the following text.

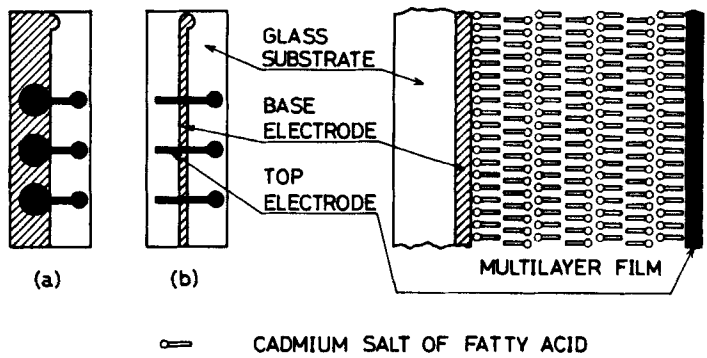

FIGURE 1 Schematic representation of the sample geometries (a) and (b), and the assembly structure. The cross section of a seven-layer assembly is shown at right.

The pH of the subphase was controlled by adding a small amount of either HCl or $KHCO_3$ to ensure conditions appropriate for C_{16}, C_{18}, C_{20} and also a mixture $(C_{16})_x$–$(C_{20})_{1-x}$ to form the *Y*-type films with the deposition ratio of approximately unity under a surface pressure of approximately 25 dyne/cm. The pH and the temperature ranges adopted for preparation extended from a pH of 6.2 ~ 6.3 for 16°C up to pH of 6.5 ~ 6.6 for 23°C.

3.2 Electrical measurements

The circuits for electrical measurements on type (a) samples are the same as given in Ref. 14. The dc and low frequency ac admittance, i.e., the conductance and the capacitance, was obtained by analyzing the Lissajous' figure.

The admittance at frequencies $\geqq 30$ Hz was measured on type (b) samples to eliminate the Maxwell–Wagner spurious effect by employing a capacitance bridge Ando TRS-10C (Ando Electric Co., Tokyo, Japan).

Each sample was stored for more than five days in a desiccator, and then measured either in a dry air or in the liquid nitrogen as described in the previous paper.[10]

4 RESULTS AND DISCUSSION

4.1 Sum rule of inverse capacitance

Figure 2 shows the inverse capacitance plotted against the number of monolayers deposited M. These data were taken on C_{16} multilayer assemblies for 10^{-3} Hz at room temperature (a) and at liquid nitrogen temperature (b). The linear relationship seen in the figure was found also for different frequencies and different monolayer species as well. This indicates that the sum rule of inverse capacitance holds in the homogeneous system, and the contribution of the individual monolayers and the oxide layers at electrode surfaces can be separated from each other.

The dielectric constants of C_{16}, C_{18} and C_{20} monolayers have been evaluated by employing the least-squares method based on the expressions,

$$1/C = 1/C'_{ox} + M/C_f, \tag{15}$$

and,

$$\varepsilon = \varepsilon_0 d C_f / 2A, \tag{16}$$

where C, C'_{ox} and C_f are the capacitances of the junction, the oxide and the monolayer, respectively, and $A = 0.200 \pm 0.003$ cm^2 is the electrode area of type (a) junction, d is the bilayer spacing given in Table I, and $\varepsilon_0 = 8.854 \times 10^{-12}$ F/m refers to the value for vacuum. The relative values for 10^{-1},

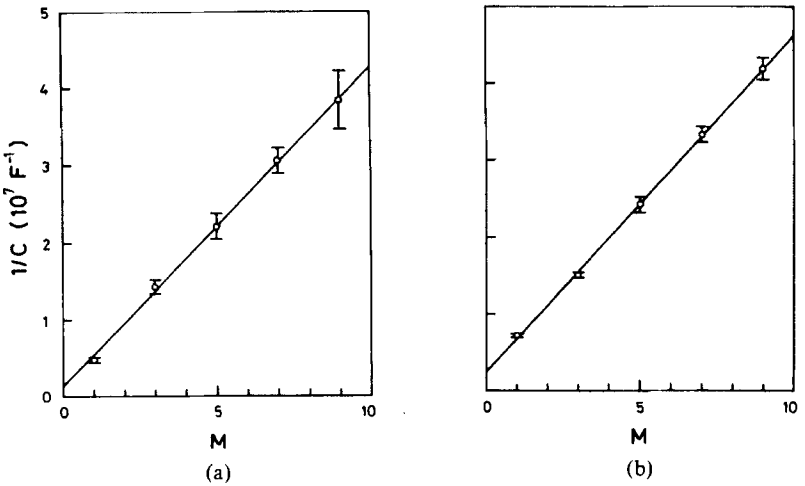

FIGURE 2 Inverse capacitance at 10^{-3} Hz of M-layer C_{16} homogeneous assembly for room temperature (a) and 77 K (b).

TABLE I

Bilayer d-spacings of Y-type Cd salt multilayers [after Ref. 5].

Constituent monolayer	Bilayer d-spacing (Å)
C_{16} (palmitate)	45.3 ± 0.1
C_{18} (stearate)	50.3 ± 0.1
C_{20} (arachidate)	55.3 ± 0.3

10^{-2} and 10^{-3} Hz are listed in Table II together with those for 1 kHz recalculated for the d values in Table I using the data of Polymeropoulos[20] and Mann and Kuhn.[21]

For each monolayer species, the dielectric constant is rather insensitive to both temperature and frequency, even up to 1 kHz. This confirms the higher stability of Cd salt multilayers, since this implies the absence of dominant relaxation process of ions in the corresponding frequency range.

4.2 Bulk ohmic relation of dc conductance

The dc conductance is subjected to the larger deviation in comparison to the capacitance, and the statistical viewpoint is indispensable to avoid the misinterpretation based on the singular cases.

TABLE II

Dielectric constants of monolayers

Monolayers	Temperature	Relative dielectric constants $\varepsilon/\varepsilon_0$			
		10^{-3} Hz	10^{-2} Hz	10^{-1} Hz	10^{3} Hz
C_{16} (palmitate)	R.T.	3.08 ± 0.12	2.93 ± 0.07	2.86 ± 0.06	2.9 ± 0.3[a]
	77 K	2.93 ± 0.06	2.92 ± 0.06	2.91 ± 0.06	
C_{18} (stearate)	R.T.	2.77 ± 0.07	2.75 ± 0.06	2.67 ± 0.05	2.64 ± 0.17[b]
	77 K	2.82 ± 0.07	2.78 ± 0.06	2.74 ± 0.06	
C_{20} (arachidate)	R.T.	2.47 ± 0.07	2.48 ± 0.05	2.44 ± 0.05	2.49 ± 0.07[b]
	77 K	2.53 ± 0.06	2.49 ± 0.05	2.48 ± 0.05	

R.T. refers to room temperature (291 to 293 K).
[a] After Polymeropoulos [Ref. 20].
[b] After Mann and Kuhn [Ref. 21].
The values are recalculated employing the d-spacings in Table I.

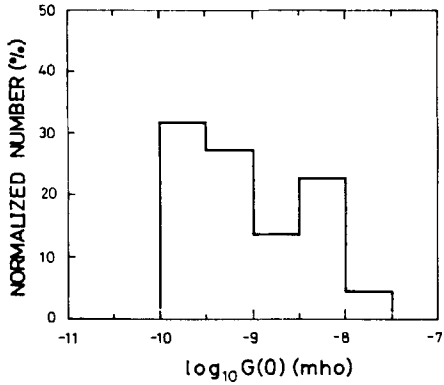

FIGURE 3 Normalized histogram of $G(0)$ at 77 K for three-layer C_{16} homogeneous assemblies.

Figure 3 shows the histogram of dc conductance at liquid nitrogen temperature for three-layer C_{16} assemblies, where the data with $G(0) > 10^{-7}$ mho (about 50% of the junctions measured) are eliminated from the statistics. Two peaks are seen even after the elimination of the short-circuited junctions, suggesting the co-existence of two different conduction mechanisms. If the main peak at the lower G(0) is assumed to be the hopping mechanism, we obtain $\langle \log_{10} G(0) \rangle = -9.42 \pm 0.29$ by eliminating the data with $G(0) > 2 \times 10^{-9}$ mho as ascribed to be due to the direct tunneling through larger pin-holes or cracks. The peak split in the histrogram and the higher occurrence of the short-circuited junctions are common features of the three-layer assemblies. For the assemblies with $M \geqq 5$, however, the histogram patterns

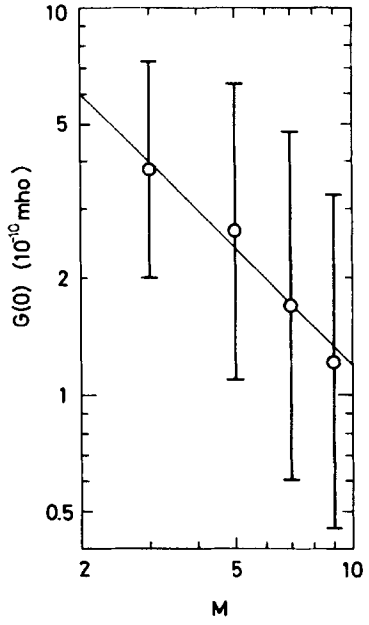

FIGURE 4 dc Conductance of C_{16} homogeneous assemblies at 77 K plotted against the layer number M.

are single peaked and fairly symmetrical in the semi-logarithmic scale, and therefore we may duly take the averages and the deviations.

Figure 4 shows G(0) of C_{16} assemblies at 77 K plotted against M in a hologarithmic scale. The straight line in the figure represents the bulk ohmic relation $G(0) \propto M^{-1}$, which is compatible with the actual behavior, although the deviations are rather large.

4.3 Exponential decrease of dc conductance with the chain length

The dc conductance of seven-layer C_n assembly is listed in Table III and also shown in Figure 5 in a semilogarithmic scale plotted against the number of carbon atoms n per acid radical, where (a) and (b) refer room temperature and 77 K, respectively. The data for 77 K were the same as reported in a previous paper,[10] but, the geometrical averages are presented here.

The exponential dependence is seen in the figure for both temperatures. The straight lines in (a) and (b), each drawn by simply connecting the averages at both extremes of n, are identical in the slope, $\partial \log_{10} G(0)/\partial n = -0.6$. Further, as already argued in the previous paper,[10] this value can be identified with the wave function damping constant $2\alpha = 1.49 \pm 0.13$ Å^{-1} ob-

TABLE III

dc Conductance of seven-layer homogeneous assemblies of C_n

Constituent monolayer	Conductance in mho			
	at Room temperature		at 77 K	
	$\log_{10} G(0)$	${}_{10}\langle \log_{10} G(0) \rangle$	$\log_{10} G(0)$	${}_{10}\langle \log_{10} G(0) \rangle$
C_{16}[a] (palmitate)	-8.60 ± 0.44	2.5×10^{-9}	-9.78 ± 0.46	1.7×10^{-10}
C_{18} (stearate)	-9.91 ± 0.53	1.2×10^{-10}	-10.83 ± 0.52	1.5×10^{-11}
C_{20}[a] (arachidate)	-11.09 ± 0.63	8.1×10^{-12}	-12.24 ± 0.57	5.7×10^{-13}

[a] After Ref. 14.

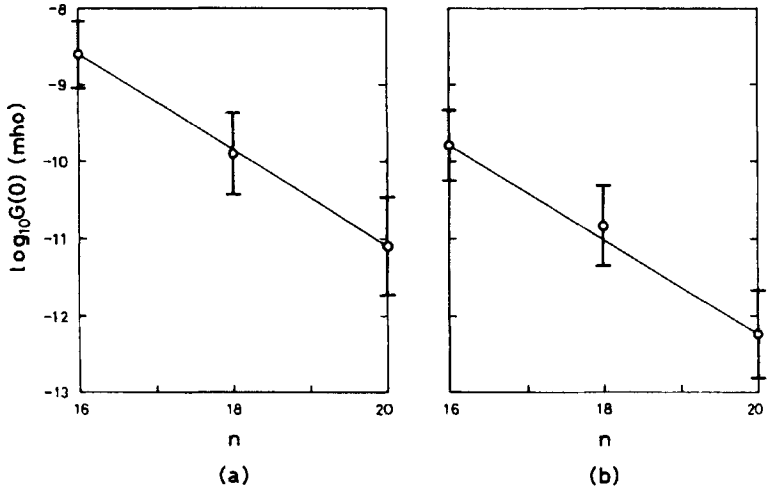

FIGURE 5 dc Conductance of seven-layer homogeneous assemblies of C_n monolayers at room temperature (a) and 77 K (b) plotted against the carbon number n.

tained by Mann and Kuhn[21] in their measurement of direct tunneling current in the single-layer junctions.

The difference of G(0) between both temperatures is about a decade for each n. The temperature-dependence is typically characterized with $T^{-1/2}$ variation as already reported.[12] These may plausibly eliminate the band conduction and the classical hopping over a potential barrier from the possible mechanisms, since in this insulative system much stronger temperature-depence should be otherwise expected.

TABLE IV

dc Conductivities of C_n multilayers

Constituent monolayer	Conductivity in mho cm^{-1}			
	At room temperature		At 77 K	
	$\log_{10} \sigma(0)$	${}_{10}\langle \log_{10} \sigma(0) \rangle$	$\log_{10} \sigma(0)\rangle$	${}_{10}\langle \log_{10} \sigma(0) \rangle$
C_{16} (palmitate)	-13.70 ± 0.44	2.0×10^{-14}	-14.88 ± 0.46	1.3×10^{-15}
C_{18} (stearate)	-14.97 ± 0.53	1.1×10^{-15}	-15.89 ± 0.52	1.3×10^{-16}
C_{20} (arachidate)	-16.10 ± 0.63	7.9×10^{-17}	-17.25 ± 0.57	5.6×10^{-18}

The dc conductivity for each n is calculated from the seven-layer conductance by assuming the bulk ohmic relation,

$$\sigma(0) = Md\mathrm{G}(0)/2A, \tag{17}$$

and listed in Table IV.

4.4 The same exponential dependence in the mixed system

The same exponential behavior is found in the mixed system $(C_{16})_x$–$(C_{20})_{1-x}$ as reported before.[11] In this case, the relation is held between the dc conductance and the average number $\langle n \rangle$. The data in the previous paper are replotted in Figure 6, where G(0) of seven-layer assembly at 77 K is shown in

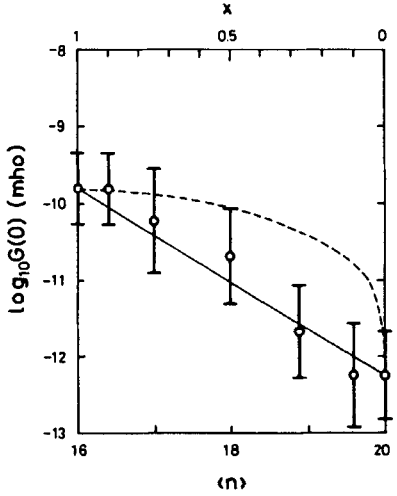

FIGURE 6 dc Conductance of seven-layer mixed system $(C_{16})_x$—$(C_{20})_{1-x}$. The solid and dashed lines correspond to the homogeneous mixing and the phase-separated cases, respectively [replotted after the data in Ref. 11].

TABLE V

dc Conductance of seven-layer homogeneous assemblies of mixed monolayers

$(C_{16})_x - (C_{20})_{1-x}$

Molar fraction x	Average number of carbon atoms $\langle n \rangle$	Conductance in mho at 77 K	
		$\log_{10} G(0)$	$_{10}\langle \log_{10} G(0) \rangle$
0[a]	20	-12.24 ± 0.57	5.7×10^{-13}
0.10	19.6	-12.24 ± 0.68	5.7×10^{-13}
0.25	19	-11.67 ± 0.61	2.1×10^{-12}
0.50	18	-10.68 ± 0.62	2.1×10^{-11}
0.75	17	-10.22 ± 0.68	6.1×10^{-11}
0.90	16.4	-9.79 ± 0.46	1.6×10^{-10}
1.00[a]	16	-9.78 ± 0.46	1.7×10^{-10}

[a] The values are taken from Table III.

a semi-logarithmic scale. The corresponding values are listed in Table V. The solid line in the figure is the same as in Figure 5(a), connecting the averages at both extremes, and now represents the relation given by Eq. (14), i.e., the homogeneous mixing case. The phase-separated case [cf. Eq. (12)] is shown by the dashed curve which does not fit to the actual behaior. It is indicated therefore that the conduction is governed by the average chain length in this system.

4.5 ac Conductance of homogeneous system

Figure 7 shows the examples of $G(\omega)$ of homogeneous seven-layer C_{16} (A), C_{18} (B) and C_{20} (C) assemblies at 77 K. Each thin solid line represents the limit of measurement corresponding to $\tan \delta = 10^{-2}$. For lower frequencies, therefore, the conductance is frequency-independent in each case in accordance with the theory [cf. Eq. (10)].

For higher frequencies, the conductance is characterized with the almost linear variation[7] as shown in Figure 8. This component is rather insensitive to both structure and constituent[22] in contrast to dc and low frequency ac conductances, and, therefore, beyond the scope of the present paper.

4.6 Reduction of dc conductance caused by one single C_{20} monolayer

The C_{20} monolayers, when incorporated in the C_{16} multilayer system with the higher conductivity, are expected to reduce rather drastically the assembly conductance.[13] This has been checked by employing the C_{16}–C_{20} heterogeneous system involving one C_{20} monolayer. The detailed description is given in a separate form,[14] and the outline is reviewed here.

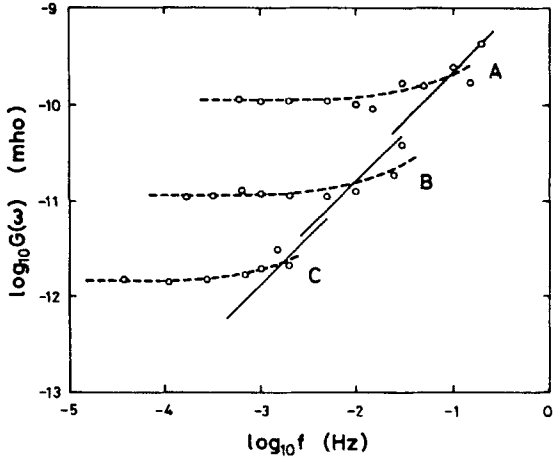

FIGURE 7 Examples of $G(\omega)$ at 77 K for seven-layer assemblies of C_{16} (A), C_{18} (B) and C_{20} (C). The thin solid lines represent $\tan \delta = 10^{-2}$, each indicating the limit of measurement for the corresponding assembly.

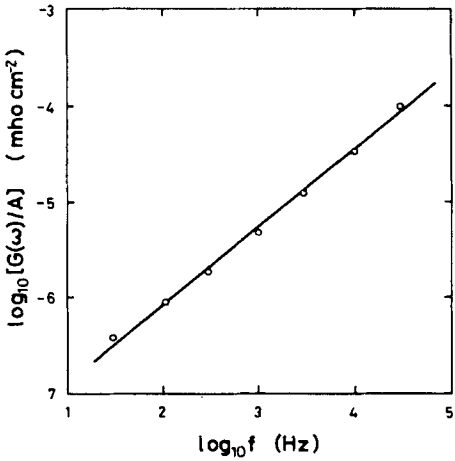

FIGURE 8 An example of the almost linear variation of $G(\omega)$. The characteristic refers to the data at room temperature taken on a type (b) junction with seven-layer C_{18} film.

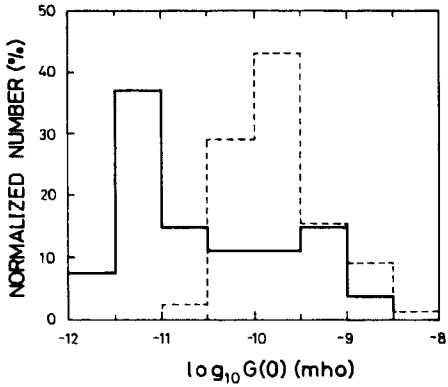

FIGURE 9 Normalized histrograms of dc conductance at 77 K of the seven-layer heterogeneous and homogeneous assemblies. The solid and dashed lines refer to the heterogeneous system with $6C_{16}$ and $1C_{20}$ monolayers and the homogeneous system $(C_{16})_{0.9}$—$(C_{20})_{0.1}$, respectively [after Ref. 14].

Figure 9 shows the histogram of G(0) at 77 K of seven-layer heterogeneous assemblies with six C_{16} and one C_{20} monolayers, i.e., $M_1 = 6$ and $M_2 = 1$ according to the notations in Sect. II. The histogram for homogeneous seven-layer assemblies of $(C_{16})_{0.9}$–$(C_{20})_{0.1}$ is also given by a dashed line for comparison, since the molar fraction $x = 0.9$ in the mixture is comparable with the layer fraction $M_1/(M_1 + M_2) = 6/7 = 0.86$ in the heterogeneous system. Two histograms are, however, rather different from each other, showing that one single C_{20} monolayer can reduce the dc conductance by a decade or even more down to the values lower than the average for C_{18} seven-layer assemblies. The dc conductance should be according to Eq. (8) identified with the seven-layer G(0) of C_{20} multiplied with 7. This is actually the case with the main peak in the histogram, and therefore affords the direct evidence of the single-layer process actually governing the multilayer conductance. If the bilayer hopping were the case, the dc level should be around the seven-layer conductance of C_{18} multiplied by 7/2, since a bilayer with a C_{16} and a C_{20} monolayers is equivalent to the C_{18} bilayer in the bilayer hopping scheme.

4.7 Conductivity-dispersion in the heterogeneous system

The frequency-dispersion of conductance has been actually observed in the heterogeneous system involving one single C_{20} monolayer as predicted by the theory. For the detailed description, the readers are referred to Ref. 14. An example is shown in Figure 10, where $G(\omega)$ and $C(\omega)$ measured on an Al(base) $[4C_{16}, 1C_{20}, 4C_{16}]$Al junction are given for room temperature (a)

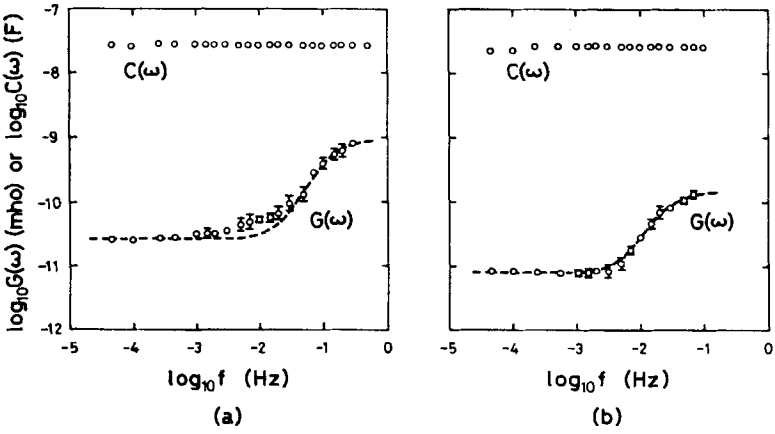

FIGURE 10 Frequency-dependence of G(ω) and C(ω) for an Al[$4C_{16}$, $1C_{20}$, $4C_{16}$]Al junction at room temperature (a) and 77 K (b) [after Ref. 14].

and 77 K (b). Each dashed line is the theoretical curves given by Eq. (8) fitted for the data. The values of the parameters are calculated by using Eqs. (4), (5) and (8)–(11), and are referred in Table VI. $G_1(0)$ and $G_2(0)$, the calculated seven-layer conductances of C_{16} and C_{20}, respectively, are within the standard deviations of the corresponding actual seven-layer conductances given in Table III. For the calculations of the common parameters N', $(\partial n/\partial\zeta)_T l$ and λ_0, we used $2a = 1.5 \times 10^8$ cm^{-1} as in the previous papers[10–12] and the corrected value of interface separation $l = 19.6 \times 10^{-8}$ cm obtained by allowing for the finite thickness of the interface region.[14]

N' and λ_0 are in agreement with those estimated before in order of magnitude. The differential carrier concentration $(\partial n/\partial\zeta)_T l$ remains constant for both temperatures. This is qualitatively in good agreement with the $T^{-1/2}$ law of conductivity variation, since the temperature-dependence of Eq. (5)

TABLE VI

Parameters calculated from the data in Figure 10 [after Ref. 14]

	At R.T.	At 77 K
$G_1(0)$ (mho)	1.30×10^{-9}	2.0×10^{-10}
$G_2(0)$ (mho)	3.9×10^{-12}	1.14×10^{-12}
λ (sec^{-1})	6.79	1.31
$(\partial n/\partial\zeta)_T l$ (eV^{-1} cm^{-2})	8.7×10^{10}	7.0×10^{10}
N' (eV^{-1} cm^{-2})	6.4×10^{15}	
λ_0 (sec^{-1})	1.4×10^{12}	

The values used for calculation are, $2a = 1.5 \times 10^8$ cm^{-1}, $l = 19.6 \times 10^{-8}$ cm for C_{16} and R.T. = 293 K.

is then represented by the hopping rate alone, which is, according to Eq. (4), characterized with the same $T^{-1/2}$ law. The magnitude is, however, by about four decades smaller than the earlier estimate based on the simplified model of degenerate electron system in which $(\partial n/\partial \zeta)_T l$ is compared with N'.[10–12] This difference in magnitude is found to be cancelled with the larger value of the actual hopping rate λ, which is rather in good agreement with the estimate based on the corrected value of l.[13]

CONCLUDING REMARKS

We have reviewed the results of electrical measurements on the Cd salt multilayer assemblies together with the theory of hopping conduction based on the single layer process in the one-dimensional array of interfaces associated with the localized electronic states. The stability of the multilayer structure in the Cd salt system has been confirmed by the sum rule of inverse capacitances of individual constituent monolayers.

The structure-dependent aspects of conductance are summarized in the following items:

1) the exponential decrease of dc conductance with the chain length of the fatty acid radicals;
2) the same exponential relation between the dc conductance and the average chain length in the mixed homogeneous system;
3) the drastic reduction of dc conductance caused by introduction of one single C_{20} monolayer into the C_{16} system;
4) the actual observation of conductivity dispersion in the heterogeneous system.

These have been appropriately explained by the single-layer hopping model.

We have said nothing about the origin of the localized states which are assumed at each interface in the model. This remains still an open question, and we cannot even deny such a possibility that those interface states are extrinsic in nature due to some unknown contaminations, while the correction of interface separation found to be appropriate seems to favor the intrinsic origin due to the end groups of the fatty acid chains.

Acknowledgments

The authors wish to thank Drs. H. Okushi and K. Tanaka for their valuable comments. They are also indebted to Prof. H. Kuhn and Dr. D. Möbius in the early stages of the research.

References

1. K. B. Blodgett, *J. Am. Chem. Soc.*, **57**, 1007 (1935).
2. H. Kuhn, D. Möbius and H. Bücher, in *Techniques of Chemistry*, Vol. I, Part III B, Eds. A. Weissberger and B. W. Rossiter (Wiley, New York, 1973).
3. For a comprehensive review, see V. K. Agarwal, *Electrocomponent Science and Technology*, **2**, 1, 75 (1975).
4. See, e.g., F. Kopp, U. P. Fringeli, K. Mühlethaler and Hs. H. Günthard, *Biophys. Struct. Mechanism*, **1**, 75 (1975).
5. T. Fukui, A. Matsuda, M. Sugi and S. Iizima, *Bul. Electrotech. Lab.*, **41**, 423 (1977).
6. M. H. Nathoo and A. K. Jonscher, *J. Phys. C*, **4**, L301 (1971).
7. M. Sugi, K. Nembach, D.Möbius and H. Kuhn, *Solid State Commun.*, **13**, 603 (1973).
8. M. Sugi, K. Nembach, D. Möbius and H. Kuhn, *Solid State Commun.*, **15**, 1687 (1974).
9. M. Sugi, K. Nembach and D. Möbius, *Thin Solid Films*, **27**, 205 (1975).
10. M. Sugi, T. Fukui and S. Iizima, *Appl. Phys. Lett.*, **27**, 559 (1975); see also **28**, 240 (1976).
11. S. Iizima and M. Sugi, *Appl. Phys. Lett.*, **28**, 548 (1976).
12. M. Sugi, T. Fukui and S. Iizima, *Chem. Phys. Lett.*, **45**, 163 (1977).
13. M. Sugi and S. Iizima, *Phys. Rev. B*, **15**, 574 (1977).
14. M. Sugi, T. Fukui and S. Iizima, *Phys. Rev. B*, **18**, 725 (1978).
15. N. F. Mott, *Phil. Mag.*, **19**, 835 (1969).
16. H. Scher and M. Lax, *Phys. Rev. B*, **1**, 4502 (1973).
17. A. Miller and E. Abrahams, *Phys. Rev.*, **120**, 745 (1960).
18. R. Kubo, *J. Phys. Soc. Jpn.*, **12**, 570 (1957).
19. E. W. Montroll and G. H. Weiss, *J. Math. Phys.*, **5**, 167 (1965).
20. E. E. Polymeropoulos, *J. Appl. Phys.*, **48**, 2404 (1977).
21. B. Mann and H. Kuhn, *J. Appl. Phys.*, **42**, 4398 (1971).
22. S. Iizima and M. Sugi, unpublished data.